Available online at www.sciencedirect.com

ScienceDirect

Journal of the Chinese Medical Association 81 (2018) 398–408

www.jcma-online.com

Original Article

Anti-atherosclerotic effect of Fermentum Rubrum and *Gynostemma pentaphyllum* mixture in high-fat emulsion- and vitamin D_3-induced atherosclerotic rats

San-Hu Gou [a], Bei-Jun Liu [a], Xiu-Feng Han [b], Li Wang [b], Chao Zhong [b], Shan Liang [b], Hui Liu [b], Yin Qiang [b], Yun Zhang [b], Jing-Man Ni [a,b,*]

[a] *Key Laboratory of Preclinical Study for New Drugs of Gansu Province, School of Basic Medical Sciences, Lanzhou University, Lanzhou, China*
[b] *School of Pharmacy, Lanzhou University, Lanzhou, China*

Received June 4, 2017; accepted August 15, 2017

Abstract

Background: The mixture of Hongqu and gypenosides (HG) is composed of Fermentum Rubrum (Hongqu, in Chinese) and total saponins of *Gynostemma pentaphyllum* (Thunb.) Makino (Jiaogulan, in Chinese) in a 3.6:1 weight ratio. Both Hongqu and Jiaogulan are considered valuable traditional Chinese medicines (TCMs); they have been commonly used in China for the treatment of hyperlipidemia and related diseases for centuries. The aim of the current study was assess the anti-atherosclerotic effect of HG.

Methods: Sixty-four Wistar rats were randomly divided into eight groups: normal, model, positive control (simvastatin, 1 mg/kg), Hongqu-treated (72 mg/kg), gypenoside (total saponin)-treated (20 mg/kg), and three doses HG-treated (50, 100, and 200 mg/kg). All of the rats were fed a basal diet. Additionally, the model group rats were intragastrically administered a high-fat emulsion and intraperitoneally injected with vitamin D_3. The serum lipid profiles, oxidative stress, inflammatory cytokine, and hepatic antioxidant levels were then determined. Furthermore, the liver histopathology and arterial tissue were analyzed, and the expression of hyperlipidemia- and atherosclerosis (AS)-related genes was measured using reverse transcription-polymerase chain reaction.

Results: The AS rat model was established after 80 days. Compared to the model group, the HG-treated groups showed an obvious improvement in the serum lipid profiles, oxidative stress, and inflammatory cytokine levels, and showed markedly increased hepatic total antioxidant capacity. Moreover, the expression of genes related to lipid synthesis and inflammation reduced and that of the genes related to lipid oxidation increased in the liver and arterial tissue, which also reflected an improved health condition.

Conclusion: the anti-atherosclerotic effects of HG were superior to those of simvastatin, Hongqu, and the gypenosides. Therefore, HG may be a useful anti-atherosclerotic TCM preparation.

Keywords: Atherosclerosis; Fermentum Rubrum; *Gynostemma pentaphyllum*; Gypenosides; Hyperlipidemia; Red yeast rice

Conflicts of interest: The authors declare that they have no conflicts of interest related to the subject matter or materials discussed in this article.

* Corresponding author. Dr. Jing-Man Ni, School of Pharmacy, Lanzhou University, Lanzhou 730000, China.
E-mail address: nijm@lzu.edu.cn (J.-M. Ni).

https://doi.org/10.1016/j.jcma.2017.08.018

1. Introduction

Atherosclerosis (AS) is characterized by chronic arterial inflammation caused by numerous factors such as dyslipidemia, neurovascular dysfunction, and oxidative stress.[1] Furthermore, it is the principal cause of cardiovascular disease (CVD), stroke, and peripheral necrosis, accounting for up to 50% of mortalities in Western countries.[2] Changing lifestyle habits of the modern society and environmental conditions have led to the development of AS at younger ages, with mortality rates due to its complications increasing yearly.[3–5]

Lipid lowering is widely recognized as an anti-AS treatment strategy. The risk of AS is greatly reduced by lowering the serum total cholesterol (TC) and triglyceride (TG) levels.[6] Therefore, excessive serum lipids, as well as high levels of oxidative stress in vivo, are also therapeutic targets of AS.[7,8] Moreover, the equal importance of anti-inflammatory and lipid-lowering therapies for AS cannot be ignored.[9,10] Consequently, the regulation of serum lipids, oxidative stress, and inflammation is an integral therapeutic regimen in the treatment of AS.

Hongqu, which is also known as red yeast rice, koji, and anka, is produced by fermenting moist, sterile rice with the yeast, *Monascus purpureus*. It is used as a food coloring agent and for brewing red yeast wine in China.[11] Modern research has shown that Hongqu contains numerous statin-like substances, and it has been used as an alternative to statins for the treatment of hyperlipidemia.[12–15] The commercial drugs, xuezhikang and zhibituo, which are red yeast rice preparations, have been clinically used to treat hyperlipidemia.[14] Gypenosides are extracts of the total saponins of Jiaogulan. The leaves of Jiaogulan are prepared from valuable and healthy teas in China.[16] Modern chemical and medical research studies have shown that Jiaogulan contains numerous dammarane-type glycosides, which are similar to ginsenosides,[17–19] and gypenosides that have shown potential in reducing the risk of cardiovascular disease, cancer, and Alzheimer's disease, and have anti-hyperlipidemic, hypoglycemic, anti-inflammatory, and antioxidant properties.[20–22] There are reports that gypenoside XLIX is an agonist of peroxisome proliferator-activated receptor (PPAR)-α.[23] This suggests that similarly to fibrates, gypenosides can reduce blood triacylglycerol levels. Both Hongqu and gypenosides potently lower cholesterol and exert antioxidant and anti-inflammatory effects. Additionally, Hongqu is “warm” while “Jiaogulan” is cold by nature according to TCM theory; the combination of “warm” and “cold” leads to “neutral,” which is more acceptable to a human body that is under the “neutral” condition, thus reducing the side effects of the medication.

In a previous study, we investigated the lipid-lowering, hepatoprotective, and atheroprotective effects of HG in hyperlipidemia by using a non-fatty liver disease (NAFLD) rat model established by administering a high-fat diet.[24] We found that HG adequately regulated blood lipids, and exhibited anti-inflammatory and anti-oxidative effects on protein molecules and enzymes, and at the genetic level.[24] In this study aimed at investigating the anti-atherosclerotic effects of HG, an atherosclerotic rat model was established by intragastric administration of a high-fat emulsion and intraperitoneal injection of vitamin D_3 (VD_3).

The anti-atherosclerotic effects of HG were evaluated mainly based on four therapeutic strategies: regulating blood lipids, anti-inflammation, antioxidant effects, and histopathological outcomes. In addition, the possible mechanisms of action were elucidated by determining the expression of genes associated with lipid synthesis and oxidation in liver tissue, as well as those associated with the development of AS in arterial tissue, by reverse transcription-polymerase chain reaction (RT-PCR).

2. Methods

2.1. Primary reagents and drugs

Hongqu (batch number: 2014012301) was purchased from Zhejiang Sanhe Bio-tech Co., Ltd., (Jiangshan, China) and the gypenosides (approval number: Z61020872) were purchased from Ankang Chia Tai Pharmaceutical Co., Ltd., (Ankang, China). VD_3 injection was produced by Shanghai General Pharmaceutical Co., Ltd., (lot: 130126), while anhydrous sodium acetate (lot: L480P65), N'N-diethyl-p-phenylene diamine sulfate (DEPPD, lot: LG90P53), and analytical-grade iron sulfate heptahydrate (lot: L5B0P40) were purchased from J&K Scientific Ltd., (Beijing, China).

2.2. Preparation and quality control of HG

HG is composed of Hongqu, gypenosides, and excipients at a weight ratio of 3.6:1:0.4. The quality control analyses of Hongqu and HG were performed using a Waters 2998 high-performance liquid chromatography (HPLC) system equipped with a Waters 1525 binary pump and photodiode array detector system. Lovastatin was used as a standard substance. The sample was separated using a Lichrospher C_{18} column (250 mm × 4.6 mm, 7-μm), and the temperature was maintained at 36 °C. The mobile phase consisted of phase A (phosphate: water = 0.1:100, v/v) and phase B (acetonitrile [ACN]). An isocratic elution was conducted with mobile phases A and B at a ratio of 35:65 (v/v). The total saponins of the gypenoside raw material and HG were determined using the vanillin-glacial acetic acid-perchloric acid method by ultraviolet visible light spectrophotometry (UV-2550, Shimadzu, Japan), and gypenoside XLIX was used as the reference substance.

2.3. Animal management and model establishment of AS

Sixty-four healthy 8-week-old adult male Wistar rats weighing 300 ± 5 g were purchased from the Lanzhou University School of Medicine, Gansu Province Key Laboratory of Drug Preclinical Research (laboratory animal certificate: scxk2013-0002). All experimental procedures were performed in accordance with the National Institutes of Health (NIH) Guide for the Care and Use of Laboratory Animals (NIH Publications No. 8023, revised 1978). The rats were housed in

an environmentally controlled room at 23 ± 1 °C and 55 ± 5% relative humidity, with a 12-h light/dark cycle and free access to water.

The rats were randomly divided into the following eight groups of eight rats per group: normal control (N), model (M), simvastatin (S, 1 mg/kg), Hongqu (H, 72 mg/kg), gypenosides (G, 20 mg/kg), and HG low-, medium-, and high-dose (HGL, HGM, and HGH, 50, 100, and 200 mg/kg, respectively). The rats were adaptively fed for 1 week before establishment of the AS model. The rats were intraperitoneally injected daily with 200,000 IU/kg of VD_3 for the first three days, followed by 150,000 IU/kg every 20 days for 80 days. During this time, the rats were fed daily with 1.5 mL/kg high-lipid emulsion via intragastric administration. The emulsion was a mixture of 75 mg/mL sugar, 45 mg/mL cholesterol, 7.5 mg/mL sodium cholate, 3 mg/mL propylthiouracil (PTU), and 15 mg/mL lard. After 80 days, the rats were anesthetized with intraperitoneal injections of chloral hydrate; all of the groups were euthanized at the same time of day to avoid circadian fluctuations.

2.4. Preparation of serum and tissue samples

Serum samples were prepared to measure biochemical parameters. Briefly, the blood samples were allowed to clot at 4 °C and then were centrifuged at 5000 g for 10 min. The serum samples were collected and stored at −20 °C until assayed. For histopathological evaluations and determinations of related enzymes and factors, the aorta and liver were stripped, and a portion of each was fixed in 10% neutral-buffered formalin at 4 °C and then stored at −80 °C until needed. The other parts of the aorta and liver used for mRNA determination were immediately placed in 10-mL sterile, RNase-free Eppendorf tubes®, and then stored at −80 °C until needed.

2.5. Serum lipid profiles

The kits for analyzing serum TC (lot: 1115041), TG (lot: 091503), low-density lipoprotein cholesterol (LDL-C, lot: 1215071), and high-density lipoprotein cholesterol (HDL-C, lot: 0315021) were produced by Sichuan Maker Biotechnology Co., Ltd., (Chengdu, China). The serum lipid profiles were determined according to the manufacturer's instructions using a biochemical autoanalyzer (Hitachi, Tokyo, Japan).

2.6. Determination of serum reactive oxygen species (ROS), malondialdehyde (MDA), nitric oxide (NO), interleukin (IL)-6, and C-reactive protein (CRP)

The assay kits for MDA (lot: 20151207), IL-6 (lot: 20151213), CRP (lot: 20151211), and NO (lot: 20151229) were purchased from Nanjing Jiancheng Bioengineering Institute (Nanjing, China); the assays were performed according to the manufacturer's instructions, using a spectrophotometric plate reader (Tecan, Männedorf, Switzerland).

Serum ROS was measured spectrofluorimetrically according to a previously reported method.[25] Briefly, 5 μL of either hydrogen peroxide (H_2O_2) standard solution or serum was added to 140 μL of 0.1 M sodium acetate buffer (pH 4.8) in each well of a 96-well microtiter plate and allowed to reach a temperature of 37 °C for 5 min. DEPPD and ferrous sulfate were separately dissolved in 0.1 M sodium acetate buffer (pH 4.8) to final concentrations of 100 μg/mL (R1) and 4.37 μM (R2), respectively. Then, 100 μL of a mixture of R1 and R2 at a ratio of 1:25, prepared immediately before use, was added to each well. The plate was preincubated at 37 °C for 1 min, and the absorbance at 505 nm was then measured for a fixed time (between 0 and 180 s) at 18-s intervals (1 unit = 1.0 mg H_2O_2/L).

2.7. Determination of antioxidant and total antioxidant capacity in liver tissue

The kits for the analyses of hepatic glutathione (GSH, lot: 20160104), superoxide dismutase (SOD, lot: 20160104), catalase (CAT, lot: 20151218), and total antioxidant capacity (TAC, lot: 20160104) were purchased from Nanjing Jiancheng Bioengineering Institute. The analyses were conducted according to the manufacturer's instructions using a spectrophotometric plate reader.

2.8. Organ index of the liver and kidney

The rat organ indexes of the liver and kidney were calculated using the following formula: organ index (%) = organ weight/body weight × 100%.

2.9. Hepatic and arterial pathological examinations

Paraffin sections of the aortic arch (4–6 μm thick) were collected and stained with hematoxylin and eosin (H&E), and frozen sections of the aortic arch and liver (5–10 μm thick) were stained with oil red O. The images were captured using a CX21 microscope (Olympus, Takachiho, Japan).

The atherosclerotic lipid plaque (the portion stained red with the oil red O staining), relative thickness of the arterial intima (the thickness ratio of the thickened intima to the arterial wall), and lipid droplets in the liver were quantified with computer image analysis using the Volocity Demo 6.0 image analyzer (Connecticut, USA).

2.10. Real-time quantitative RT-PCR (qRT-PCR)

Total RNA was extracted from the liver and abdominal aorta using RNAiso Plus reagent (Takara Bio-Technology Co., Ltd., Dalian, China). Reverse transcription was performed using a PrimeScript RT Master Mix cDNA synthesis kit (Takara Bio. Inc., Otsu, Shiga, Japan). The qRT-PCR was performed with SYBR® Premix Ex TaqTM II (Takara Bio. Inc., Otsu, Shiga, Japan) using the Corbett Research Rotor-Gene RG 3000 Real Time PCR system (Corbett Research, Hilly Street, Mortlake NSW 2137, Australia) as previously reported.[24]

The reverse transcription reaction volume of 10 μL contained 500 ng total RNA. The primers used are described in

Table 1. The reactions were performed with 10 μL of SYBR® Premix Ex TaqTM II, 1.6 mL of 10 mM primer pairs, 6 mL of distilled water, 0.4 μL of Rox reference dye (50×), and 2 μL of cDNA. Each PCR run was performed under the following conditions: initial denaturation at 95 °C for 30 s, 40 cycles at 95 °C for 15 s, and renaturation at 60 °C for 30 s. The gene expression levels were compared with those of β-actin as a reference gene.

2.11. Statistical analysis

The experimental data are expressed as means ± standard deviations (SDs). Values were compared with one-way analysis of variance (ANOVA) using the statistical package for the social sciences (SPSS) 16.0 (IBM, Armonk, NY, USA). Differences were considered significant at $p < 0.05$.

3. Results

3.1. Main ingredients and content of raw material and HG

The main active ingredient of Hongqu, lovastatin, was detected at a content of 30.658 mg/g in Hongqu raw material. Furthermore, the total Jiaogulan saponins were the main active ingredients, and their content was 820 mg/g of gypenoside XLIX in the gypenosides raw material. Within HG, the content of lovastatin and total Jiaogulan saponins was 22.07 and 200 mg/g, respectively.

3.2. Blood lipid-regulating effect of HG

After 80 days, the serum TC, TG, and LDL-C levels of the model group were higher, and the HDL-C level was lower than those in the normal group (Fig. 1). These results suggest that the hyperlipidemia model was successfully established. Compared to the model group, all of the treated groups showed significant amelioration of blood lipid levels. Moreover, the serum TG-lowering effect of the medium HG dose (1.44 mM) was superior to that of simvastatin (1.66 mM) ($p < 0.05$), but the TC- and LDL-C-lowering and HDL-C-elevating effects of the medium HG dose were similar to those of simvastatin ($p > 0.05$). Furthermore, HG normalized blood lipid levels better than Hongqu or the gypenosides alone did ($p < 0.05$). The blood lipid-regulating effect of HG was dose-dependent.

3.3. Anti-inflammatory and antioxidant effects of HG

As shown in Fig. 2, the serum IL-6 and CRP levels in the model group increased while the NO levels decreased compared with those of the normal group ($p < 0.01$). These effects were obviously prevented by treatment with different doses of HG ($p < 0.01$). The positive control drug, simvastatin, decreased the serum IL-6 levels, but had no therapeutic effect on serum NO and CRP levels. In addition to the effects on CRP, the effects of HG on NO and IL-6 were dose-dependent and superior to those of Hongqu and the gypenosides ($p < 0.05$ and $p < 0.01$, respectively). For unknown reasons, the low HG dose reduced CRP levels more than the medium HG dose did, indicating that, at least for CRP, HG does not elicit a standard dose-response.

As shown in Fig. 3, the serum ROS and MDA levels of the model group increased compared with those of the normal group ($p < 0.01$ and $p < 0.05$, respectively). The serum ROS and MDA levels were markedly decreased by the treatments with gypenosides and HG, but Hongqu and simvastatin had no effect on the serum ROS level ($p > 0.05$ for both). The effect of lowering serum ROS and MDA was better with HG than with Hongqu or the gypenosides ($p < 0.05$). However, the magnitude of the effect was small.

To investigate the antioxidant capacity further, the GSH, CAT, SOD, and TAC levels of the liver tissue samples were

Table 1
Oligonucleotide polymerase chain reaction (PCR) primers for target genes.

Gene	GenBank accession number	Gene sequences (5′-3′)	
		Forward	Reverse
β-actin	NM_031144.3	GGAGATTACTGCCCTGGCTCCTA	GACTCATCGTACTCCTGCTTGCTG
HMGR	NM_013134.2	TGGCAGGACGCAACCTCTAC	AATAGTTACCACTGACCGCCAGAA
PPAR-α	NM_013196.1	GGCAATGCACTGAACATCGAG	GCCGAATAGTTCGCCGAAAG
FAS	NM_017332.1	GCTGCTACAAACAGGACCATCAC	TCTTGCTGGCCTCCACTGAC
ACC-1	NM_022193.1	CAATCCTCGGCACATGGAGA	GCTCAGCCAAGCGGATGTAGA
CPT-1	NM_031559.2	AGGTCGGAAGCCCATGTTGTA	GCTGTCATGCGCTGGAAGTC
SREBP-1c	NM_001276707.1	CCCTGCGAAGTGCTCACAA	GCGTTTCTACCACTTCAGGTTTCA
NOS_2	NM_012611.3	TTCAGGTCACCTTGGTAGGATTTG	TCCTCAGGCTTGGGTCTTGTTAG
ICAM-1	NM_012967.1	ATGAGGTTCTTGCCCACCTG	GCTTCTGCCACCATCACTGTGTA
TNF-α	NM_012675.3	GTTGTCTTTGAGATCCATGCCATT	TCAGTTCCATGGCCCAGAC
IL-6	NM_012589.2	ATTGTATGAACAGCGATGATGCAC	CCAGGTAGAACGGAACTCCAGA
MCP-1	NM_031530.1	CTATGCAGGTCTCTGTCACGCTTC	CAGCCGACTCATTGGGATCA
CCL-5	NM_031116.3	ACCAGCAGCAAGTGCTCCAA	AGCTGGTTAGGACTAGAGCAAGCAA
NF-κB	NM_199267.2	CGACGTATTGCTGTGCCTTC	TTGAGATCTGCCCAGGTGGTA

3-hydroxy-3-methylglutaryl coenzyme A reductase (*HMGR*); peroxisome proliferator-activated receptor (*PPAR*)-α; fatty acid synthase (*FAS*); acetyl-CoA carboxylase (*ACC*)-*1*; carnitine palmitoyl transferase (*CPT*)-*1*; sterol response element-binding protein (*SREBP*)-*1c*; inducible nitric oxide synthase (NOS_2); intercellular adhesion molecule (*ICAM*)-*1*; tumor necrosis factor (*TNF*)-α; interleukin (*IL*)-6; monocyte chemotactic protein (*MCP*)-1; chemokine (C–C motif) ligand (*CCL*)-*5*; nuclear factor (*NF*)-κ*B*.

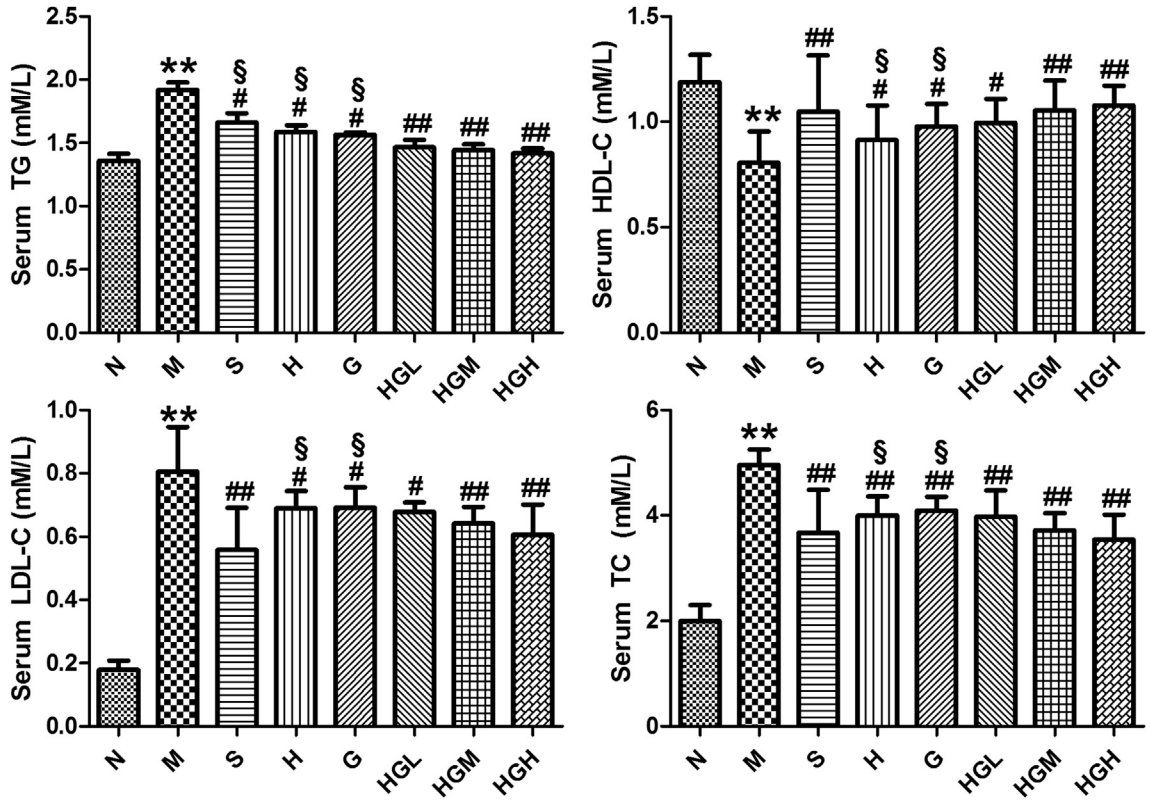

Fig. 1. Effect of 50-day intervention treatment on serum triglyceride (TG), high-density lipoprotein-cholesterol (HDL-C), low-density lipoprotein-cholesterol (LDL-C), and total cholesterol (TC) levels of various rat groups. Groups: N: normal, M: model, S: simvastatin (1 mg/kg), H: Hongqu (72 mg/kg), G: gypenosides (20 mg/kg), HGL, HGM, and HGH: Hongqu and gypenosides low (50 mg/kg), medium (100 mg/kg), and high (200 mg/kg), respectively. $^{**}p < 0.01$, M vs. N; $^{\#\#}p < 0.01$ and $^{\#}p < 0.05$, S, H, G, HGL, HGM, and HGH vs. M; $^{\S}p < 0.05$, S, H, and G vs. HGM (n = 8, mean ± SD).

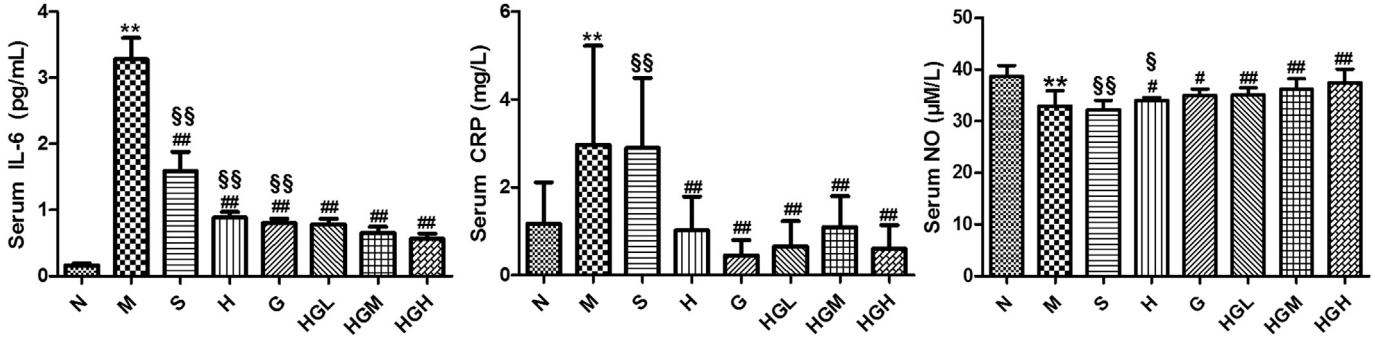

Fig. 2. Effect of 50-day intervention treatment on serum inflammatory factors, interleukin (IL)-6, C-reactive protein (CRP), and nitric oxide (NO) of rats. Groups: N: normal, M: model, S: simvastatin (1 mg/kg), H: Hongqu (72 mg/kg), G: gypenosides (20 mg/kg), HGL, HGM, and HGH: Hongqu and gypenosides low (50 mg/kg), medium (100 mg/kg), and high (200 mg/kg), respectively. $^{**}p < 0.01$, M vs. N; $^{\#\#}p < 0.01$ and $^{\#}p < 0.05$, S, H, G, HGL, HGM, and HGH vs. M; $^{\S\S}p < 0.01$ and $^{\S}p < 0.05$, S, H, and G vs. HGM (n = 8, mean ± SD).

determined. Compared with those of the normal group, the TAC levels of the model group were decreased and the SOD seems to had a reduced representation from the column chart, but this had no statistically significant, while the GSH levels were dramatically increased and the CAT seems to had a increased representation from the column chart, as well, it had no statistically significant. The medium and high dose of HG treatments increased the CAT, SOD, and TAC levels more than those of the model group. However, the GSH levels were considerably decreased (Fig. 4).

3.4. Organ index and pathological analysis

As shown in Fig. 5, the kidney index of the simvastatin group was slightly elevated. Compared with that of the normal group, the kidney indexes of the other groups did not show a statistically significant change. The liver index of the model group increased markedly compared with that of the normal group. The relative increase in the liver weight was inhibited by treatment with the drugs, simvastatin, Hongqu, gypenosides, and HG.

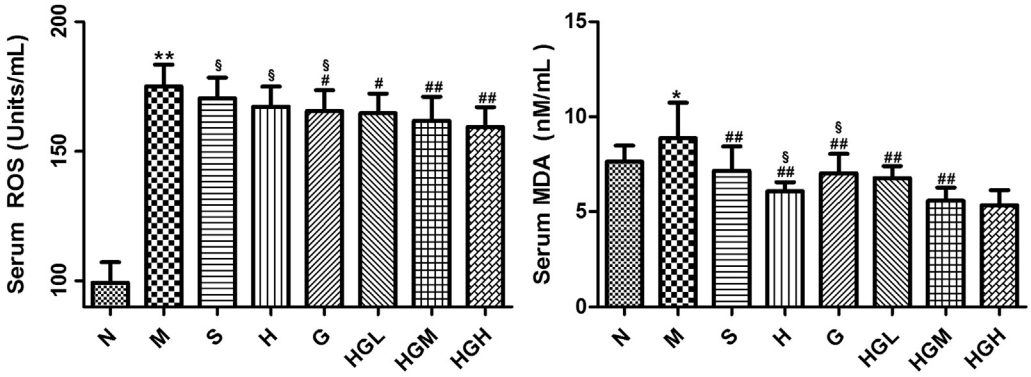

Fig. 3. Effect of 50-day intervention treatment on serum reactive oxygen species (ROS) and malondialdehyde (MDA) levels of model rat groups established after 80 days. Groups: N: normal, M: model, S: simvastatin (1 mg/kg), H: Hongqu (72 mg/kg), G: gypenosides (20 mg/kg), HGL, HGM, and HGH: Hongqu and gypenosides low (50 mg/kg), medium (100 mg/kg), and high (200 mg/kg), respectively. $^{**}p < 0.01$ and $^{*}p < 0.05$, M vs. N; $^{\#\#}p < 0.01$ and $^{\#}p < 0.05$, S, H, G, HGL, HGM, and HGH vs. M; $^{\S\S}p < 0.01$ and $^{\S}p < 0.05$, S, H, and G vs. HGM (n = 8, mean ± SD).

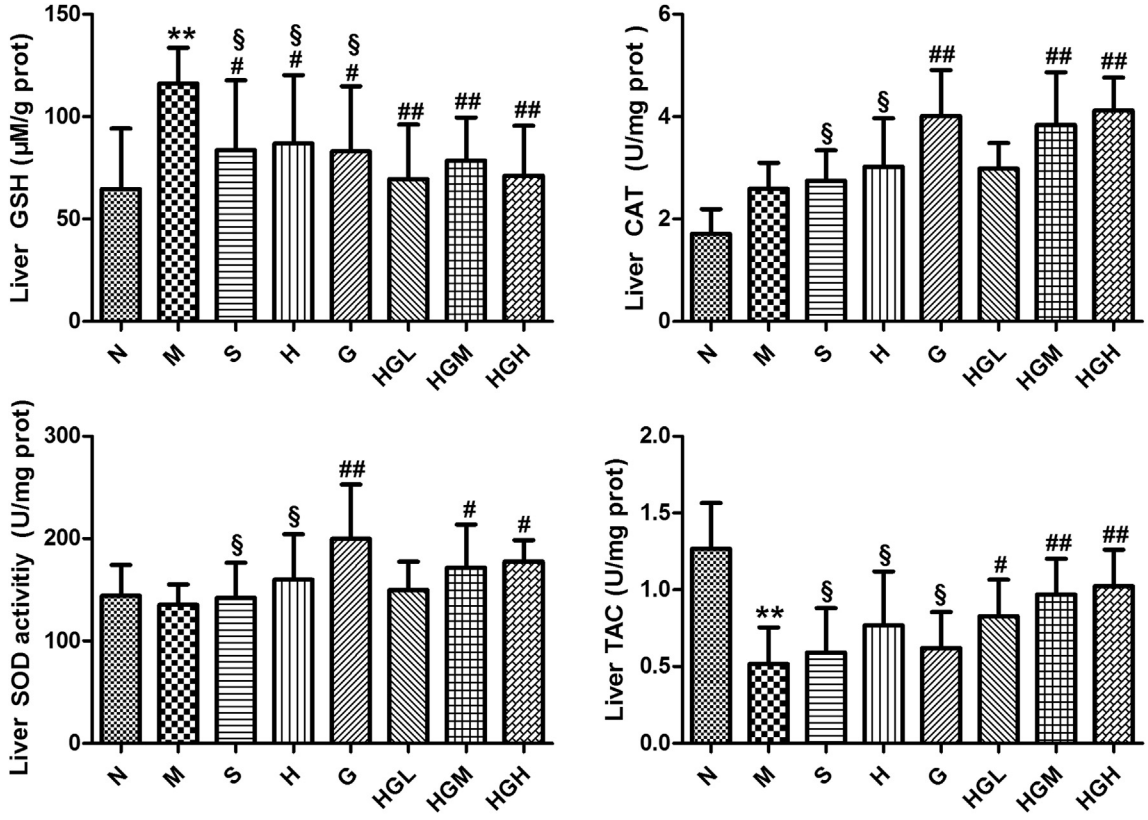

Fig. 4. Liver glutathione (GSH), catalase (CAT), superoxide dismutase (SOD), and total antioxidant capacity (TAC) levels of eight rat groups after intervention treatment for 50 days. Group: N: normal, M: model, S: simvastatin (1 mg/kg), H: Hongqu (72 mg/kg), G: gypenosides (20 mg/kg), HGL, HGM, and HGH: Hongqu and gypenosides low (50 mg/kg), medium (100 mg/kg), and high (200 mg/kg), respectively. $^{**}p < 0.01$ and $^{*}p < 0.05$, M vs. N; $^{\#\#}p < 0.01$ and $^{\#}p < 0.05$, S, H, G, HGL, HGM, and HGH vs. M; $^{\S\S}p < 0.01$ and $^{\S}p < 0.05$, S, H, and G vs. HGM (n = 3, mean ± SD).

In the histopathological liver sections stained with oil red O (Fig. 6A and B), the round fat droplets in the intercellular and intracellular compartments of the liver cells were clearly visible. The round fat droplets were barely discernible in the normal and HGH groups and a lot of red fat droplets were presented in the model group. In Fig. 6B, The HG groups showed a significant, dose-dependent improvement in hepatic lipid accumulation compared with that of the other treatment groups.

The rats in the model group exhibited obvious symptoms of AS in the aortic histopathological sections. There was evidence of thickening of the arterial intima, disordered arrangement of the smooth muscle and elastic fibers, red foam cells, fatty plaques, and deposition of calcium in the sections stained with H&E and oil red O. The other groups were normal except for the gypenosides group, which showed adipose tissue and mild intimal thickening in the sections stained with oil red O (Fig. 7A–C).

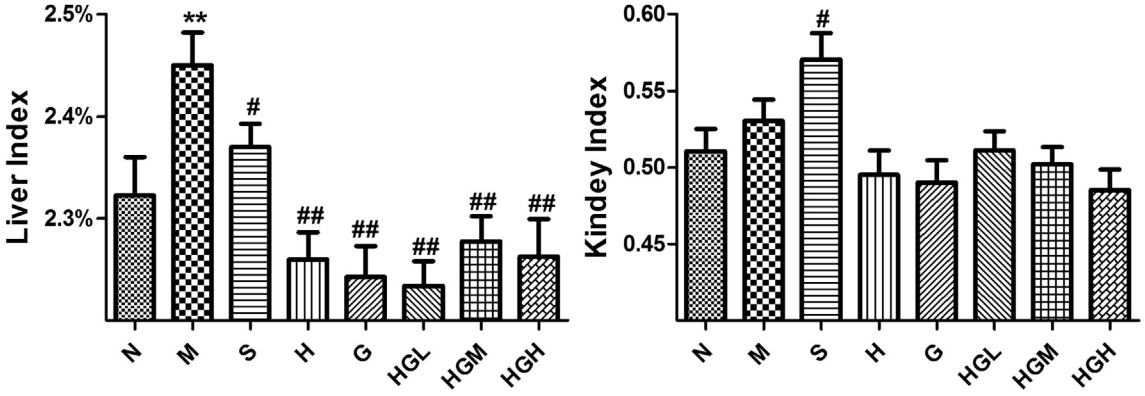

Fig. 5. Organ indexes of liver and kidney. Rats organ indexes of liver and kidney were calculated using the following formula: organ index = organ weight/body weight × 100%. Groups: N: normal, M: model, S: simvastatin (1 mg/kg), H: Hongqu (72 mg/kg), G: gypenosides (20 mg/kg), HGL, HGM, and HGH, Hongqu and gypenosides low (50 mg/kg), medium (100 mg/kg), and high (200 mg/kg), respectively. $^{*}p < 0.05$, M vs. N; $^{\#\#}p < 0.01$ and $^{\#}p < 0.05$, S, H, G, HGL, HGM, and HGH vs. M (n = 8, mean ± SD).

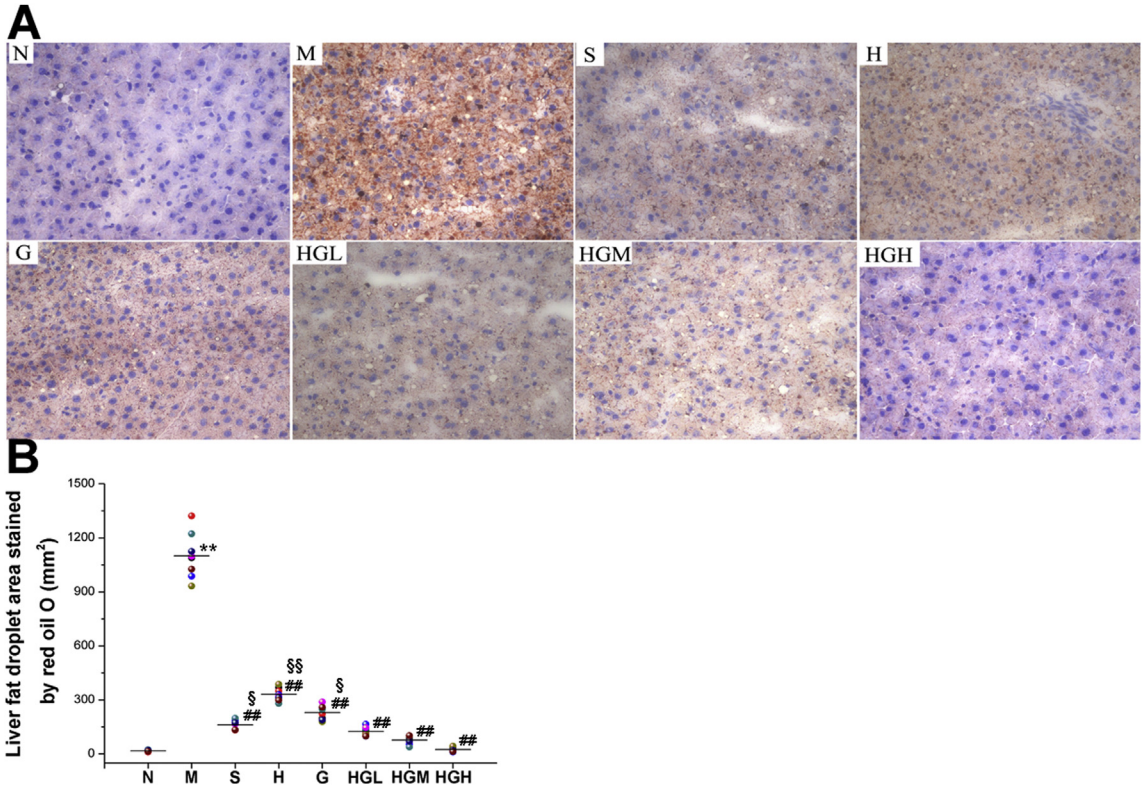

Fig. 6. Photomicrographs of liver sections after model establishment for 80 days and intervention treatment for 50 days. (A) Sections stained with oil red O (400×). (B) Liver fat droplet areas stained with red oil O from each group were quantified using computer-assisted morphometry. $^{**}p < 0.01$, M vs. N; $^{\#\#}p < 0.01$, S, H, G, HGL, HGM, and HGH vs. M; $^{\S\S}p < 0.01$ and $^{\S}p < 0.05$, S, H, and G vs. HGM. Groups: N: normal, M: model, S: simvastatin (1 mg/kg). H: Hongqu (72 mg/kg), G: gypenosides (20 mg/kg), HGL, HGM, and HGH: Hongqu and gypenosides low (50 mg/kg), medium (100 mg/kg), high (200 mg/kg), respectively.

3.5. Gene expression in liver and aorta

As shown in Fig. 8A, the hepatic gene expressions of 3-hydroxy-3-methylglutaryl coenzyme A reductase (HMGR), fatty acid synthase (FAS), and sterol response element-binding protein-1c (SREBP-1c) were significantly inhibited by simvastatin compared with those of the model group, but including the acetyl-CoA carboxylase-1 (ACC-1), HG had the same effects as simvastatin. Furthermore, except for HMGR, HG showed better inhibition trends of gene expression than simvastatin did but that had not statistically significant. Hongqu and gypenosides showed a synergistic inhibitory effect on HMGR and ACC-1 gene expression. Simvastatin had no significant effect on the expression of peroxisome proliferator-activated receptor α (PPAR-α) and carnitine palmitoyl transferase-1 (CPT-1), while Hongqu had no obvious effect on

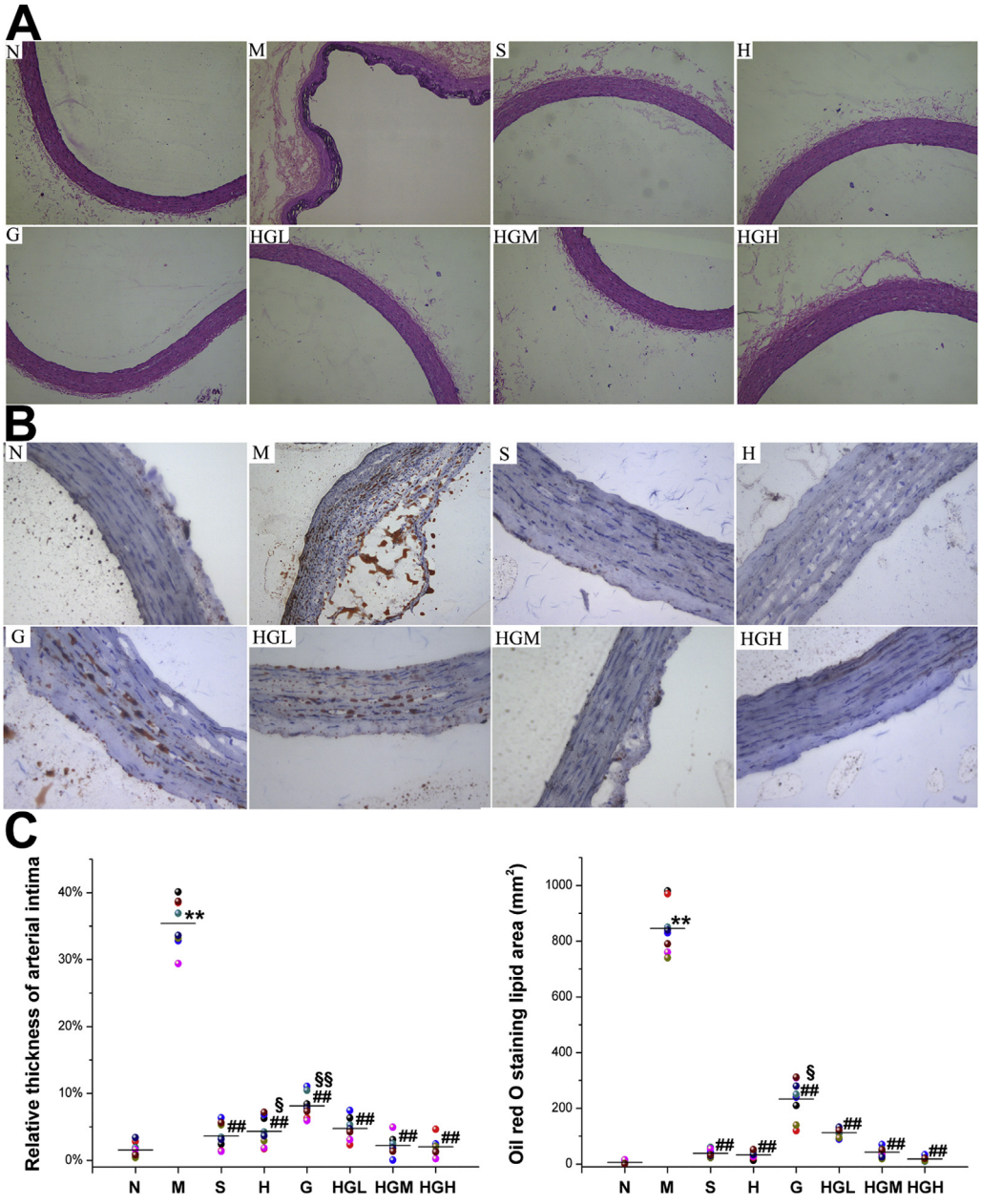

Fig. 7. Photomicrographs of aorta sections from rat model established for 80 days and administered intervention treatment for 50 days. (A) Sections stained with hematoxylin and eosin (H&E, 100×). (B) Sections stained with oil red O and hematoxylin (400×). (C) Thickness (%) of arterial intima in whole aortic arch and oil red O-stained aortic lipid areas from each group were quantified using computer-assisted morphometry. $^{**}p < 0.01$, M vs. N; $^{\#\#}p < 0.01$, S, H, G, HGL, HGM, and HGH vs. M; $^{\S\S}p < 0.01$ and $^{\S}p < 0.05$, S, H, and G vs. HGM. Groups: N: normal, M: model, S: simvastatin (1 mg/kg), H: Hongqu (72 mg/kg), G: gypenosides (20 mg/kg), HGH, HGM, HGL: Hongqu and gypenosides low (50 mg/kg), medium (100 mg/kg), and high (200 mg/kg), respectively.

the expression of PPAR-α. HG, the mixture of Hongqu and the gypenosides significantly improved the expression of various genes compared with Hongqu or the gypenosides, therefore Hongqu and the gypenosides showed a synergistic effect. Moreover, except for HMGR, HG showed a dose-dependent trends regulatory effect on the genes analyzed in the liver.

Genes involved in the development of AS were analyzed in the aorta (Fig. 8B). The expression of inducible nitric oxide synthase (NOS_2) did not change significantly after modeling and treatment. The suppressive effect of HG on the expression of other genes was significantly greater than that of simvastatin, especially on intercellular adhesion molecule-1 (ICAM-1), tumor necrosis factor-α (TNF-α), and IL-6. Moreover, except for the medium- and high-dose HG, the drugs did not have significant effects on monocyte chemotactic protein-1 (MCP-1). Apart from MCP-1, Hongqu and gypenoside did not show a significant, synergistic inhibitory effect on the expression of other genes.

4. Discussion

Investigations of animal models of AS currently focus on using rodents, especially gene knockout animals such as ApoE-deficient and LDL receptor gene knockout mice.[26]

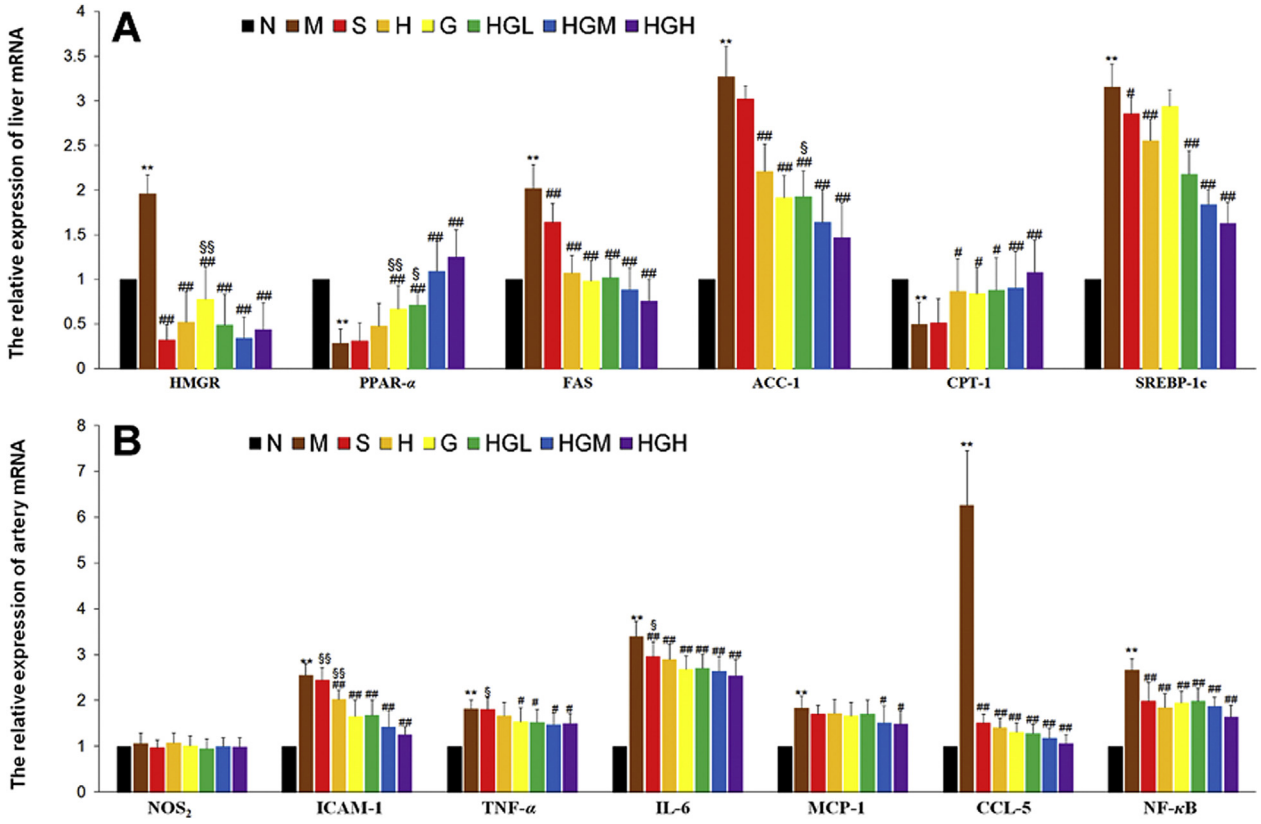

Fig. 8. mRNA expression levels in liver and artery. mRNA expression in (A) liver (HMGR, PPAR-α, FAS, ACC-1, CPT-1, SREBP-1c) and (B) artery (NOS_2, ICAM-1, TNF-α, IL-6, MCP-1, CCL-5, NF-κB). Data were normalized to the gene expression of the untreated, N group. $^{**}p < 0.01$, M vs. N; $^{\#\#}p < 0.01$ and $^{\#}p < 0.05$, S, H, G, HGL, HGM, and HGH vs. M; $^{\S\S}p < 0.01$ and $^{\S}p < 0.05$, S, H, and G vs. HGM (n = 8, mean ± SD). Groups: N: normal, M: model, S: simvastatin (1 mg/kg), H: Hongqu (72 mg/kg), G: gypenosides (20 mg/kg), HGH, HGM, HGL: Hongqu and gypenosides low (50 mg/kg), medium (100 mg/kg), and high (200 mg/kg), respectively.

Furthermore, feeding a high-fat diet to the animals contributes to AS induction.[26] In the present study, we used VD_3 and high-fat emulsion to induce AS in the rat model, which has also been reported.[27] VD_3 may play a critical role in increasing arterial calcification and inducing smooth muscle proliferation.[28] The advantage of the high-fat emulsion over a solid high-fat diet is that the content of the lipid emulsion fed to the animals is controllable, and the animals are free to eat basic diets. The high-fat emulsion effectively induced AS in the rats and shortened the time and cost of modeling.

Arterial intimal thickening, the presence of foam cells, and the formation of lipid plaques are considered significant pathological features of AS.[29] In the present study, the pathological changes of the model group were as follows: atherosclerotic lesions such as arterial intimal thickening and calcification, evidenced by H&E staining; arterial smooth muscle proliferation; and elastic fiber arrangement disorder. Oil red O, a lipid-specific staining reagent clearly identified arterial lipid plaques and foam cells. These indicators showed that the AS rat model was successfully established.

Mononuclear macrophages internalize oxidized LDL, and their embedment in the arterial intima causes the pathological changes associated with AS.[30] The presence of excessive levels of cholesterol in the blood or peripheral cells, or dysfunctional metabolism in addition to the presence of ROS increases the risk of AS further.[31] In this current study, HG reduced the risk of AS to a large extent by reducing serum cholesterol, TG, and ROS levels. Moreover, the gene expression of HMGR was inhibited, which subsequently reduced the synthesis of endogenous cholesterol. The serum lipid and LDL-C levels of the AS rats were significantly reduced while their HDL-C levels were increased after treatment with HG. In addition, the quantification of liver genes revealed that HG inhibited not only HMGR but also ACC-1, FAS, and the cholesterol synthesis regulator, SREBP-1c. The expressions of PPAR-α and CPT-1 genes, which are related to lipid oxidative metabolism, were also enhanced. Therefore, from upstream lipid synthesis to downstream lipid oxidation, serum lipid levels were reduced by HG in numerous ways.[32]

In addition, the activities of antioxidant enzymes in the liver (i.e., SOD and CAT) were increased after treatment with HG. Although GSH may have been reduced in vivo because of the strong antioxidant capacity or feedback regulation of the drug, the in vivo TAC increased significantly after HG treatment. These results were also confirmed by the measurement of serum levels of MDA, which is the final product of lipid peroxidation. The lipid and oxidative stress levels were increased after the model was established, but the serum MDA

level was significantly reduced by treatment with HG.[33] These results suggest that HG influenced in vivo oxidative stress.

The disease progression of AS is driven by inflammatory reactive responses. Many of the molecules, such as TNF-α, IL-1β, IL-2, IL-6, IL-8, IL-12, NOS_2, cyclooxygenase (COX)-2, chemokines, adhesion molecules, and colony-stimulating factors, involved in the early stages of the immune response and in various stages of the inflammatory response are regulated by nuclear factor-κB (NF-κB).[34] Monocytes/macrophages infiltrate throughout each process in the development of atherosclerotic lesions, while the chemokines MCP-1 and CCL-5 induce the migration of monocytes via ICAM-1.[35–37] Furthermore, ICAM-1 and vascular cell adhesion molecule (VCAM)-1 mediate the adhesion of monocytes and lymphocytes to endothelial cells as well as the penetration of monocytes through the endothelial cells into the vessel wall. These adhesion molecules also protect monocytes from apoptosis. Collectively, these processes result in early vascular endothelial cell damage.[35–37]

TNF-α is a proinflammatory cytokine produced mainly by activated monocytes and macrophages, and it has multiple effects. TNF-α is involved in promoting the expression of adhesion molecules, recruiting and activating inflammatory cells, and promoting the development of AS by affecting lipid metabolism. Dyslipidemia can be induced by TNF-α for a prolonged period, which increases cardiovascular morbidity and mortality.[38] In addition, TNF-α increases the instability of plaques.[38] Inflammatory mediators such as IL-6 regulate the process of inflammation, promote monocyte proliferation and differentiation, and promote the expression of CRP.[39,40] Moreover, CRP is a marker of inflammation that is closely related to the development of atherosclerosis. CRP activates immune cells, induces proliferation of vascular smooth muscle cells, and directly induces arterial inflammation.[41] In the present study, HG not only decreased the expression of NF-κB, but also decreased the expressions of TNF-α, MCP-1, and ICAM-1 in the arterial tissue, and decreased CRP and IL-6 levels in the serum. The reduction in the expressions of these proinflammatory molecules had physiological significance because monocyte migration, adhesion, and differentiation in the arterial wall were effectively inhibited.

NOS_2 facilitates the immune system actions of macrophages against pathogens by generating NO oxidative stress (i.e., free radicals). NO also relaxes smooth muscle and regulates the inflammatory response.[42] After the AS model was established, serum NO content decreased, but it slightly increased after the drug treatment, which would be expected to relax the vascular smooth muscle and, thereby, protect the arterial endothelium to a certain extent. However, the gene expression of NOS_2 did not show any significant difference after modeling and treatment, suggesting that these actions did not involve NOS_2, and serum NO may have been regulated by endothelial nitric oxide synthase (NOS_3) or neuronal nitric oxide synthase (NOS_1).[43]

The results of the histopathological analyses showed that the vascular inflammation, thickening of the arterial wall, proliferation of the smooth muscle and foam cells, and lipid plaques appeared to be due to oxidative stress. In addition, the serum cholesterol accumulation and lipid metabolism disorder were increased in the model rats. Furthermore, the liver also showed varying degrees of fatty lesions, including direct fatty degeneration of the liver cells into larger fat cells, or liver cells with small fat particles. These can be detected by staining arterial and liver sections with H&E and oil red O. The histological sections from the treatment groups appeared almost normal, but the anti-atherosclerotic effect of other treatment groups (S, H, HGL, HGM and HGH) more effective than gypenosides (the group of G). In particular, after HG high-dose treatment, the AS lesions were completely absent.

In conclusion, HG, which is composed of Hongqu and gypenosides, not only has excellent blood lipid-lowering effects but also has potent anti-inflammatory and antioxidant capacities. This reduces lipid synthesis, increases lipid oxidation and metabolism, and reduces the incidence of vascular inflammation at the level of mRNA transcription either in the present AS rat model or in the previous hyperlipidemia with NAFLD rat model. Therefore, HG effectively repairs the atherosclerotic and fatty liver lesions via multiple action mechanism (regulating blood lipids, anti-inflammatory and antioxidant, et al.), and may be a potential candidate for developing therapeutic options for AS.

Acknowledgments

This study was supported by the National Natural Science Fund of China (81273440) and the Science and Technology Pillar program fund of Gansu Province (1204FKC151).

References

1. Carlos G, Santos G, Belen P, Juan JB. Pathophysiology of acute coronary syndrome. *Curr Atheroscler Rep* 2014;**16**:1–9.
2. Chen L, Hong Y, Hui JY, Ding SH, Fan YL, Pan YH, et al. Global transcriptomic study of atherosclerosis development in rats. *Gene* 2016;**592**:43–8.
3. Wu SW, Yang D, Wei HY, Wang B, Huang J, Li HY, et al. Association of chemical constituents and pollution sources of ambient fine particulate air pollution and biomarkers of oxidative stress associated with atherosclerosis: a panel study among young adults in Beijing, China. *Chemosphere* 2015;**135**:347–53.
4. Barth JD. Diet did not die. Just another diet study or? *Atherosclerosis* 2016;**251**:534–5.
5. Shah RV, Murthy VL, Allison MA, Ding J, Budoff M, Frazier-Wood AC, et al. Diet and adipose tissue distributions: the multi-ethnic study of atherosclerosis. *Nutr Metab Cardiovasc Dis* 2016;**26**:185–93.
6. Isles CG, Paterson JR. Identifying patients at risk for coronary heart disease: implications from trials of lipid-lowering drug therapy. *QJM* 2000;**93**:567–74.
7. Afonso MS, Lavrador MS, Koike MK, Cintra DE, Ferreira FD, Nunes VS, et al. Dietary interesterified fat enriched with palmitic acid induces atherosclerosis by impairing macrophage cholesterol efflux and eliciting inflammation. *J Nutr Biochem* 2016;**32**:91–100.
8. Papageorgiou N, Tousoulis D. Oxidized-LDL immunization for the treatment of atherosclerosis: how far are we? *Int J Cardiol* 2016;**222**:93–4.
9. Chistiakov DA, Orekhov AN, Bobryshev YV. Immune-inflammatory responses in atherosclerosis: role of an adaptive immunity mainly driven by T and B cells. *Immunobiology* 2016;**221**:1014–33.
10. Delaney JA, Lehmann N, Jöckel KH, Elmariah S, Psaty BM, Mahabadi AA, et al. Associations between aspirin and other non-steroidal anti-inflammatory drugs and aortic valve or coronary artery calcification:

the Multi-Ethnic Study of Atherosclerosis and the Heinz Nixdorf Recall Study. *Atherosclerosis* 2013;**229**:310−6.
11. Zhang Z, Ali Z, Khan SI, Khan IA. Cytotoxic monacolins from red yeast rice, a Chinese medicine and food. *Food Chem* 2016;**202**:262−8.
12. Avula B, Cohen PA, Wang YH, Sagi S, Feng W, Wang M, et al. Chemical profiling and quantification of monacolins and citrinin in red yeast rice commercial raw materials and dietary supplements using liquid chromatography-accurate QToF mass spectrometry: chemometrics application. *J Pharm Biomed Anal* 2014;**100**:243−53.
13. Childress L, Gay A, Zargar A, Ito MK. Review of red yeast rice content and current Food and Drug Administration oversight. *J Clin Lipidol* 2013;**7**:117−22.
14. Xie X, Wang Y, Zhang S, Zhang G, Xu Y, Bi H, et al. Chinese red yeast rice attenuates the development of angiotensin II-induced abdominal aortic aneurysm and atherosclerosis. *J Nutr Biochem* 2012;**23**:549−56.
15. Yoshioka E, Uto H, Yanagisawa C, Machida N, Kishimoto Y, Hasegawa M, et al. We-P14:394 Inhibition of LDL oxidation in red yeast rice. *Atheroscler Suppl* 2006;**7**:433−4.
16. Tsai TH, Tsai TH, Chien YC, Lee CW, Tsai PJ. In vitro antimicrobial activities against cariogenic streptococci and their antioxidant capacities: a comparative study of green tea versus different herbs. *Food Chem* 2008;**110**:859−64.
17. Zhao Y, Xie Z, Niu Y, Shi H, Chen P, Yu LL. Chemical compositions, HPLC/MS fingerprinting profiles and radical scavenging properties of commercial *Gynostemma pentaphyllum* (Thunb.) Makino samples. *Food Chem* 2012;**134**:180−8.
18. Yang F, Shi H, Zhang X, Yang H, Zhou Q, Yu LL. Two new saponins from tetraploid jiaogulan (*Gynostemma pentaphyllum*), and their anti-inflammatory and α-glucosidase inhibitory activities. *Food Chem* 2013;**141**:3606−13.
19. Chiranthanut N, Teekachunhatean S, Panthong A, Khonsung P, Kanjanapothi D, Lertprasertsuk N. Toxicity evaluation of standardized extract of *Gynostemma pentaphyllum* Makino. *J Ethnopharmacol* 2013;**149**:228−34.
20. Zhao Y, Niu Y, Xie Z, Shi H, Chen P, Yu LL. Differentiating leaf and whole-plant samples of di- and tetraploid *Gynostemma pentaphyllum* (Thunb.) Makino using flow-injection mass spectrometric fingerprinting method. *J Funct Foods* 2013;**5**:1288−97.
21. Šamec D, Valek-Žulj L, Martinez S, Grúz J, Piljac A, Piljac-Žegarac J. Phenolic acids significantly contribute to antioxidant potency of *Gynostemma pentaphyllum* aqueous and methanol extracts. *Ind Crops Prod* 2016;**84**:104−7.
22. Zou C, Shi H, Liu X, Sheng Y, Ding T, Yan J, et al. Conjugated linolenic acids and nutraceutical components in Jiaogulan (*Gynostemma pentaphyllum*) seeds. *LWT-Food Sci Technol* 2016;**68**:111−8.
23. Huang TH, Li Y, Razmovski-Naumovski V, Tran VH, Li GQ, Duke CC, et al. Gypenoside XLIX isolated from *Gynostemma pentaphyllum* inhibits nuclear factor-kappaB activation via a PPAR-alpha-dependent pathway. *J Biomed Sci* 2006;**13**:535−48.
24. Gou SH, Huang HF, Chen XY, Liu J, M1 He, Ma YY, et al. Lipid-lowering, hepatoprotective, and atheroprotective effects of the mixture Hong-Qu and gypenosides in hyperlipidemia with NAFLD rats. *J Chin Med Assoc* 2016;**79**:111−21.
25. Hayashi I, Morishita Y, Imai K, Nakamura M, Nakachi K, Hayashi T. High-throughput spectrophotometric assay of reactive oxygen species in serum. *Mutat Res* 2007;**631**:55−61.
26. Li D, Liu Y, Zhang X, Lv H, Pang W, Sun X, et al. Inhibition of soluble epoxide hydrolase alleviated atherosclerosis by reducing monocyte infiltration in Ldlr−/− mice. *J Mol Cell Cardiol* 2016;**98**:128−37.
27. Pang J, Xu Q, Xu X, Yin H, Xu R, Guo S, et al. Hexarelin suppresses high lipid diet and vitamin D_3-induced atherosclerosis in the rat. *Peptides* 2010;**31**:630−8.
28. Norman PE, Powell JT. Vitamin D and cardiovascular disease. *Circ Res* 2014;**114**:379−93.
29. Aprahamian TR, Zhong X, Amir S, Binder CJ, Chiang LK, Al-Riyami L, et al. The immunomodulatory parasitic worm product ES-62 reduces lupus-associated accelerated atherosclerosis in a mouse model. *Int J Parasitol* 2015;**45**:203−7.
30. Nash KM, Ahmed S. Nanomedicine in the ROS-mediated pathophysiology: applications and clinical advances. *Nanomedicine* 2015;**11**:2033−40.
31. Park SH, Hur SK, Yoo JY, Jeong SJ, Oh GT. Increased mitochondrial ROS accelerate atherosclerosis in mitochondrial catalytic enzyme 3 deficient mice. *Atherosclerosis* 2016;**252**:220.
32. Choi WH, Gwon SY, Ahn J, Jung CH, Ha TY. Cooked rice prevents hyperlipidemia in hamsters fed a high-fat/cholesterol diet by the regulation of the expression of hepatic genes involved in lipid metabolism. *Nutr Res* 2013;**33**:572−9.
33. Omari-Siaw E, Wang Q, Sun C, Gu Z, Zhu Y, Cao X, et al. Tissue distribution and enhanced in vivo anti-hyperlipidemic-antioxidant effects of perillaldehyde-loaded liposomal nanoformulation against Poloxamer 407-induced hyperlipidemia. *Int J Pharm* 2016;**513**:68−77.
34. Yates LL, Górecki DC. The nuclear factor-kappaB (NF-kappaB): from a versatile transcription factor to a ubiquitous therapeutic target. *Acta Biochim Pol* 2006;**53**:651−62.
35. Safa A, Rashidinejad HR, Khalili M, Dabiri S, Nemati M, Mohammadi MM, et al. Higher circulating levels of chemokines CXCL10, CCL20 and CCL22 in patients with ischemic heart disease. *Cytokine* 2016;**83**:147−57.
36. Cortes R, Ivorra C, Martínez-Hervás S, Pedro T, González-Albert V, Artero A, et al. Postprandial Changes in Chemokines Related to Early Atherosclerotic processes in familial hypercholesterolemic subjects: a preliminary study. *Arch Med Res* 2016;**47**:33−9.
37. Čejková S, Králová-Lesná I, Poledne R. Monocyte adhesion to the endothelium is an initial stage of atherosclerosis development. *Cor Vasa* 2016;**58**:419−25.
38. Jiang W, Cen Y, Song Y, Li P, Qin R, Liu C, et al. Artesunate attenuated progression of atherosclerosis lesion formation alone or combined with rosuvastatin through inhibition of pro-inflammatory cytokines and pro-inflammatory chemokines. *Phytomedicine* 2016;**23**:1259−66.
39. Bernberg E, Ulleryd MA, Johansson ME, Bergström GM. Social disruption stress increases IL-6 levels and accelerates atherosclerosis in ApoE−/− mice. *Atherosclerosis* 2012;**221**:359−65.
40. Yoshida M, Higashi K, Kobayashi E, Saeki N, Wakui K, Kusaka T, et al. Correlation between images of silent brain infarction, carotid atherosclerosis and white matter hyperintensity, and plasma levels of acrolein, IL-6 and CRP. *Atherosclerosis* 2010;**211**:475−9.
41. Morrison M, van der Heijden R, Heeringa P, Kaijzel E, Verschuren L, Blomhoff R, et al. Epicatechin attenuates atherosclerosis and exerts anti-inflammatory effects on diet-induced human-CRP and NFκB *in vivo*. *Atherosclerosis* 2014;**233**:149−56.
42. Liu Z, Wildhirt SM, Weismüller S, Schulze C, Conrad N, Reichart B. Nitric oxide and endothelin in the development of cardiac allograft vasculopathy. Potential targets for therapeutic interventions. *Atherosclerosis* 1998;**140**:1−14.
43. Oliveira-Paula GH, Lacchini R, Tanus-Santos JE. Clinical and pharmacogenetic impact of endothelial nitric oxide synthase polymorphisms on cardiovascular diseases. *Nitric Oxide* 2017;**63**:39−51.